ELEMENTA
Science of the Anthropocene

Korbeń, P, et al. 2022. Quantification of methane emission rate from oil and gas wells in Romania using ground-based measurement techniques. *Elem Sci Anth*, 10: 1. DOI: https://doi.org/10.1525/elementa.2022.00070

RESEARCH ARTICLE

Quantification of methane emission rate from oil and gas wells in Romania using ground-based measurement techniques

Piotr Korbeń[1,*], Paweł Jagoda[2], Hossein Maazallahi[3], Johannes Kammerer[1], Jarosław M. Nęcki[2], Julia B. Wietzel[1], Jakub Bartyzel[2], Andrei Radovici[4], Daniel Zavala-Araiza[3,5], Thomas Röckmann[3], and Martina Schmidt[1,*]

The ROMEO campaign (ROmanian Methane Emissions from Oil and gas) focused on measurements of methane (CH_4) emission rates from oil and natural gas (O&G) production in Romania. The campaign took place in October 2019 and covered the southern part of Romania around the cities Bucharest, Ploiesti, Pitesti, and Craiova. This study presents emission rates calculated from mobile in situ measurement of CH_4 and wind measurements using the Other Test Method 33a from U.S. Environmental Protection Agency and the Gaussian Plume Method. These methods were used to determine emission rates from 112 O&G well sites and other production-related facilities. Estimated mean CH_4 emission rate with a 95% confidence interval equals 0.49 [0.35, 0.71] kg CH_4 h^{-1} per site; 10% of all quantified sites account for 56% of the estimated emission rates. In addition, more than 1,000 O&G sites were visited for a qualitative "screening" (CH_4 detection without quantification). Analysis of the screening data shows that 65% of the sites emitted methane at detectable rates. The CH_4 emission rates obtained during the ROMEO campaign are comparable to the methane emission rates in study carried out in other Romanian regions.

Keywords: Methane, Oil and gas, Gaussian plume, Greenhouse gas, Mobile measurements, Fossil fuels

Introduction

Methane is, after carbon dioxide, the most important greenhouse gas, with natural and anthropogenic emission sources (U.S. Environmental Protection Agency [EPA], 2016). The short atmospheric lifetime of methane of about 10 years and the approximately 80 times stronger global warming potential than CO_2 on a 20 years' time scale makes it an essential candidate for climate change mitigation in parallel to CO_2 (Intergovernmental Panel on Climate Change, 2021; Ocko et al., 2021).

According to recent studies, methane emissions from the oil and gas sector range from 80 to 140 Tg CH_4/year (Schwietzke et al., 2016; Saunois et al., 2019; Hmiel et al., 2020). Reductions of CH_4 emissions associated with oil and natural gas (O&G) production, processing, and transport are considered as relatively easy-to-implement solutions that can often be achieved at low cost today compared with other anthropogenic CH_4 sources like the agriculture or waste sectors (International Energy Agency, 2017; Ocko et al., 2021).

Over the last decade, many studies on the quantification of methane emission rates from oil and gas supply chain have been carried out in the United States (Mitchell et al., 2015; Yacovitch et al., 2015; Zavala-Araiza et al., 2015; Allen, 2016; Omara et al., 2018; Robertson et al., 2020) and a few additional countries like Canada (Zavala-Araiza et al., 2018; Ravikumar et al., 2020; Tyner and Johnson, 2021), Mexico (Shen et al., 2021), in Middle East and Mediterranean areas (Paris et al., 2021), or globally (Lauvaux et al., 2022). However, in other regions, even in Europe, there are only limited studies that quantified emission rates from oil and gas producing sectors (Cain et al., 2017; Yacovitch et al., 2018; Delre et al., 2022).

The emission rates reported for the year 2018 to the United Nations Framework Convention on Climate Change (UNFCCC) show that Romania, Germany, and Italy are the countries in the European Union with the highest CH_4 annual emissions from the oil and gas sector (UNFCC,

[1] Institute of Environmental Physics, Heidelberg University, Heidelberg, Germany
[2] Faculty of Physics and Applied Computer Science, AGH—University of Science and Technology in Kraków, Kraków, Poland
[3] Institute for Marine and Atmospheric research Utrecht, Utrecht University, Utrecht, the Netherlands
[4] Faculty of Environmental Science and Engineering, Babeş-Bolyai University, Cluj-Napoca, Romania
[5] Environmental Defense Fund, Reguliersgracht, Amsterdam, the Netherlands

* Corresponding authors:
Emails: pkorben@iup.uni-heidelberg.de; korbenpiotr@gmail.com; martina.schmidt@iup.uni-heidelberg.de

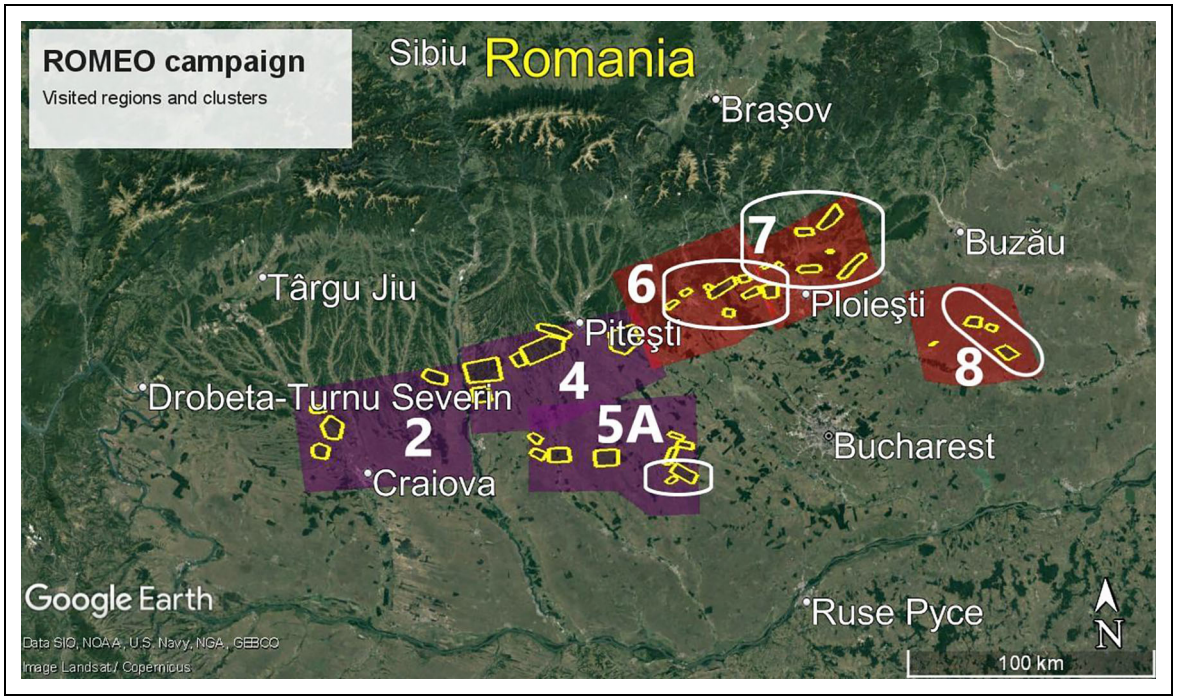

Figure 1. Map of the target regions of the ROMEO campaign (Google ©). Sites were grouped in big regions (violet color—2, 4, and 5A; red color—6, 7, and 8), and small clusters in each region, which were areas with a high density of oil and gas wells (yellow polygons). More detailed figures are available in Figure S1. The white enclosures were studied in the paper of Delre et al. (2022). ROMEO = ROmanian Methane Emissions from Oil and gas.

https://di.unfccc.int/detailed_data_by_party). Romania alone contributes 13% to the European CH_4 emissions from the oil and gas-production sector. However, this information is highly uncertain (Solazzo et al., 2021) as the reported emission rates are calculated using standard emission factors (i.e., not specific to the O&G technologies and practices used in Romania as a whole or production subregions in particular), and independent measurements of methane emission rates from oil and gas production in Romania are lacking. In order to address this gap of knowledge, the ROmanian Methane Emissions from Oil and gas project (ROMEO) set out to quantify emission rates using atmospheric measurements. From September 30 until October 20, 2019, a 3-week measurement campaign with up to 70 participants from 14 research institutes was carried out in Southern Romania.

From the measurements carried out during the ROMEO campaign, two studies have already been published and more are in preparation. Delre et al. (2022) investigated CH_4 emission rates from the oil and gas sector North of Bucharest using a tracer dispersion method. The CH_4 emission rates are reported with a 95% confidence interval (CI) equal to 0.53 [0,32, 0.79] kg CH_4 h^{-1} and site. The study of Menoud et al. (2022) focused on the CH_4 isotope composition of the sites visited during the ROMEO campaign. In addition, there will be an overview ROMEO paper relating to the upscaling of the obtained values for the entire ROMEO campaign.

In this study, we present the results of mobile in situ measurements performed with 5 cars equipped with methane analyzers from Heidelberg University, AGH Krakow, and Utrecht University in cooperation with National Institute for Aerospace Research "Elie Carafoli" (INCAS; Bucharest, Romania) and UBB (Cluj-Napoca; Romania). Two of the cars were dedicated to "screening," that is, to locate possible methane emitters and to identify appropriate locations for further quantifications according to the requirements for the Other Test Method 33a (OTM-33a) and Gaussian Plume Method (GPM) performed by the crew of the remaining 3 cars. The measured data sets were processed centrally at University Heidelberg to apply a Gaussian Plume Model or the OTM-33a method algorithm (U.S. EPA; Thoma and Squier, 2014) to calculate methane emission rates for individual oil and gas facilities. The screening data were used to estimate the number of CH_4 emission rates below the detection limit and to integrate the information obtained in this study.

Materials and methods

Mobile atmospheric in situ measurements during the ROMEO campaign were mainly focused on the southern region of Romania, close to the cities of Bucharest, Ploiesti, Pitesti, and Craiova. **Figure 1** shows a map section of Romania, with regions and clusters, corresponding to areas with a high density of oil and gas wells. The clusters cover areas between 2 and 120 km^2 and contain between 10 and 530 oil and gas wells and other production related facilities like oil parks (an installation where oil from numerous individual wells in the surroundings is collected) or compressor stations. Mobile CH_4 measurements were carried out by three research groups: Institute of Environmental Physics of Heidelberg University (UHEI, Germany), Faculty of Physics and Applied Computer Science of AGH University of Science and Technology in

Table 1. Specification of in situ analyzers used for quantification and screening including methane (Licor Manual, LGR Manual, Picarro G4301) and meteorology measurements

Species	UHEI_1	AGH_1	UU	UHEI_2[a]	AGH_2[a]
Instrument	LI-7810	LGR M-GGA-918	1. Picarro G4301; 2. Picarro G2401	Picarro G1301	Picarro G2201-i
Measured species	CH_4, CO_2, H_2O	CH_4, CO_2, H_2O	1. CH_4, C_2H_6, H_2O; 2. CH_4, C_2H_6, H_20, CO	CH_4, CO_2	CH_4, CO_2, H_20
Measurement interval [s]	1	1	1. 12. <5		
<5	<4				
Precision (1 s, CH_4)	<1 ppb	4 ppb	1. 30 ppb 2. <1 ppb		5 ppb (30 s average)
3D Windsensor	METEK Ultrasonic anemometer USA-1	Three-axis ultrasonic anemometer "Young, Model 81000V"	Campbell Scientific CSAT3 3D Sonic Anemometer	—	TriSonica™ Mini Wind and Weather Sensor
2D Windsensor	Gill MaxiMet GMX500	—	Gill MaxiMet GMX200	—	—

[a]Screening-only cars.

Kraków (AGH, Poland), and Institute for Marine and Atmospheric research Utrecht of Utrecht University (UU, the Netherlands). These teams were equipped with cars, drivers, and support staff from INCAS and UBB (Babes-Bolyai University), who also supported integration of the instruments.

Instrumentation and measurement vehicles

The UHEI research group in cooperation with UBB and INCAS equipped 2 cars with in situ methane analyzers. The equipment of the cars is described in detail below for vehicle UHEI_1, while the equipment of the other vehicles is summarized in **Table 1** and Table S1. UHEI_1 was equipped with a high-precision Optical Feedback—Cavity-Enhanced Absorption Spectroscopy analyzer (Licor Li-7810, LI-COR, Inc., https://www.licor.com/env/products/trace_gas/LI-7810#specs) to measure CH_4 and CO_2 mole fraction in ambient air. This device recorded data with 1-Hz measurement rate, precision (1σ) better than 1-ppb CH_4 at ambient mole fraction, and a drift lower than 1 ppb per 24-h period. It was mainly used for quantification using the OTM-33a or Gaussian plume modeling approach. The air inlet line was mounted at the roof rack 2.5 m above ground with a funnel to protect the line against rain water. Air was flushed through the inlet line, a particle filter, and the analyzer at a flow rate of 250 mL/min, resulting in a delay time from the inlet to the cell of the analyzer of typically 8 s. This delay time was measured each day, before the start of the measurements and used for proper data time stamp correction during evaluation process to synchronize the data of methane analyzer, GPS (precision of 3 m) and weather station. Meteorological data were collected with 2 anemometers: a 2D weather station (Gill MaxiMet GMX500, Gill, Lymington, UK) and a 3D sonic anemometer (USA-1, Metek, Germany). The 2D weather station was mounted on the roof rack and recorded temperature, humidity, pressure, wind speed and wind direction, and GPS coordinates during driving. The software, provided by the manufacturer, allowed retrieving the wind speed and direction while driving. The 3D sonic anemometer was installed on a portable tripod and set to a height of 2.5 m, which corresponds to the inlet height of the car. When performing transects for Gaussian plume modeling or stationary measurements downwind of the plume, the 3D sonic anemometer was installed close by. Geographic coordinates of the car were recorded by a 2D weather station in addition to the GPS logger application (BasicAirData GPS Logger, precision of 3 m) installed on a smart phone. It was used to determine the exact position of the analyzer during stationary measurements. In some cases, the downwind methane plume was not accessible by car; then, the lightweight CH_4 analyzer (Li-7810) was installed outside the car next to the 3D sonic anemometer.

The second car (UHEI_2) was equipped with a cavity ring down spectrometer (CRDS, Model G1301, Picarro Inc.). As we had no additional weather station and the data acquisition frequency of the analyzer was only 0.2 Hz, this device was deployed for the screening of potential emitters.

The other 3 cars were equipped by UU and AGH using the same measurement methods and setups as UHEI_1 but with different instrumentation. **Table 1** summarizes the methane and meteorological sensors of the five measurement vehicles used during the campaign. A detailed description of each mobile setup is included in Table S1.

CH_4 calibration scale

All the methane analyzers were calibrated at the beginning of the ROMEO campaign with gas mixtures from 10 different high-pressure cylinders spanning a methane

mole fraction range between 2 and 130 ppm (Table S2). The high CH_4 mole fraction of most of these cylinders is outside of international calibration scales (Dlugokencky et al., 2005). Therefore, the scale of the calibration gases was checked at Groningen University by dilution experiments and a common scale was established for the ROMEO campaign. Based on the reported data for the calibration tanks, the data from all instruments were harmonized to this scale, using instrument-specific calibration functions provided by Groningen University. During the campaign, the analyzers were calibrated at least once per day using one of the high-pressure cylinders to detect and apply possible correction.

Site selection

When planning the campaign, the measurement area was divided into regions and clusters based on information about the coordinates of the sites provided by the oil and gas operator of the production facilities in the studied regions. It was planned that the measurement teams spent 3–4 days in one of the 6 regions shown in **Figure 1** before moving to the next one. The selection of the measurement sites, or clusters, was random and optimized to visit as many sites as possible, but to avoid double measurements by two different groups. Based on the weather forecast, clusters of potential sites were preselected each morning. The "screening cars" UHEI_2 and AGH_2 drove from site to site, circling the oil/gas well if possible, and measured the mole fraction downwind of the wells, taking notes on accessibility, CH_4 mole fraction above background, obstacles and determining whether nearby wells could affect subsequent emission quantifications. UU used one additional instrument for occasional screening and emission quantification measurements as well as to collect air samples for isotope analysis (Menoud et al., 2022). The site selection for an OTM-33a or Gaussian plume measurement was based on the following criteria: a methane enhancement of at least 200 ppb above ambient background level during screening (see Section: Gaussian Plume Model and OTM-33a), appropriate wind direction (to allow downwind sampling from a public road), no obstacles that could influence the dispersion of the plume, suitable access of the terrain for measurements. All measurements were carried out during daytime (between 9 AM and 5 PM) with a typical duration between 20 and 70 min at each site.

A total of 1,043 sites (wells and facilities) were screened on the 20 measurement days with 5 cars; 85% of these sites were oil, while 10% were gas production sites. The rest was other facility, not marked in the table by local oil and gas operator. Of these, 112 sites were visited at least once for more detailed quantification and evaluated using the OTM-33a or GPM.

GPM

We used the GPM to estimate CH_4 emission rates from downwind mobile transects through a plume originating from an emission site. This method has been used in recent studies (e.g., Yacovitch et al., 2015; Ars et al., 2017; Caulton et al., 2018; Kammerer, 2019; Kumar et al., 2021). When a site was identified as suitable for GPM (path perpendicular to wind direction, detected clear methane signal), then 5–22 measurement transects were performed downwind the source. Hereby, we recorded individual realizations of the emission plume and compared them to the results of the GPM, which provides a theoretical approximation of the average CH_4 dispersion on a local scale under the assumption of constant meteorological conditions in time and space over a flat terrain (Ars et al., 2017; Omara et al., 2018; Kumar et al., 2021). The formula for Gaussian plume dispersion given in Equation 1 (Turner, 1970) provides a relation between the emission rate Q and the maximum observed mole fraction C, requiring information on the distance and height of the emitter relative to the sensor and the local meteorological parameters

$$C(x,y,z) = \frac{Q}{2\pi\sigma_y\sigma_z U}\exp\left(-\frac{1}{2}\left(\frac{y}{\sigma_y}\right)^2\right)\left[\exp\left(-\frac{1}{2}\left(\frac{z-H}{\sigma_z}\right)^2\right) + \exp\left(-\frac{1}{2}\left(\frac{z+H}{\sigma_z}\right)^2\right)\right], \quad (1)$$

where y is the distance from the plume center point, x is the downwind distance between emission location and measurement transect, and z and H are the measurement and release heights, respectively (Figure S2). U is the average wind speed and σ_y and σ_z are the horizontal and vertical dispersion coefficients (calculated based on the Briggs parametrization during plume capture and downwind distance, x, from the site [Table S3; Hanna et al., 1982; Griffiths, 1994]). The incoming solar radiation and wind speed allow for the determination of atmospheric stability class (A–D, Table S4). The background CH_4 mole fractions were calculated as a mean of the 5% lowest CH_4 values measured during the transects driven at the selected sites (5–22 transects). The transect length was chosen to cover sufficient background values before and after the peak. The background calculation, driving speed, wind averaging, and other parameters were examined during several release experiments (Korbeń, 2021). This background was subtracted from the measured methane mole fraction to derive the enhancement above background. The average wind speed, U, was calculated separately for each plume crossing, which usually lasted between 30 and 60 s. The wind direction was calculated based on geographic coordinates for the highest methane mole fraction in relation to the coordinates of the emitter, following Kumar et al. (2021). Since the output of GPM is linear with respect to Q, we set the initial emission rate Q to 1 g/s to model the corresponding methane mole fraction C. Similar to the study of Kumar et al. (2021), we used the integral of the mole fraction above the background within a transect as well as the integral of the modeled peak. The ratio between model and actual mole fraction corresponds to the estimated emission rate in g/s (Mønster et al., 2014; Kammerer, 2019).

As a criterion for a good comparison between measured and modeled plume for each transect, the calculated coefficient of determination R^2 greater than 0.5 was used

to accept transects. In addition, each individual peak was inspected to exclude cases with unfavorable trajectories, like when the car was turning too early, and the part of peak was cut. Only transects that pass the quality check were included in the average emission rate for a given emitter. Estimated emission rates were calculated with an R script, using Equation 1 and all steps described above (Kammerer, 2019). The GPM model code and the quality criteria were validated with controlled release experiment to check the accuracy of the method (Korbeń, 2021). The results of four release test performed during 3 years show that the combined mobile measurements with GPM work within an accuracy of $\pm 30\%$. This finding is in agreement of other studies (Caulton et al., 2018; Kumar et al., 2021).

OTM-33a

OTM-33a is a method developed by the U.S. EPA (www.epa.gov). It is described in detail and applied in Brantley et al. (2014), Thoma et al. (2015), Robertson et al. (2017), Omara et al. (2018), Edie et al. (2020), and Robertson et al. (2020). The concept is based on stationary measurements of mole fraction of a trace gas as a function of the wind direction. This is similar to a Gaussian Plume Model, but instead of moving a detector through a plume, changes in wind direction move the plume across a stationary detector, and thus, the Gaussian plume is formed after taking into account the gas transport. The methane analyzer and 3D weather station were set up at a distance of 20–200 m from the source in the main wind direction and measured for at least 15–20 min. For 1-Hz data, this results in at least 900–1,200 data points for the data processing. For analysis, wind speed and direction, as well as the atmospheric stability class (point Gaussian indicator [PGI]), were determined from the meteorological measurements. The PGI values were calculated using the standard deviation of the wind direction and the standard deviation in vertical wind speed (turbulent intensity) following the EPA guideline (Table S5). Based on measured source distance and the averaged PGI, the horizontal and vertical dispersion coefficients, σ_y and σ_z, respectively, were determined (OTM-33a, EPA; Thoma and Squier, 2014). The average methane background mole fraction was calculated using the lowest 5% of measured CH_4 values and subtracted from all methane mole fraction data to derive enhancements above background. Then, the CH_4 enhancements were averaged as a function of the wind direction in 10° bins. Bins containing less than 2% of the total number of points were set to 0-ppm CH_4 enhancement. The peak methane mole fraction was determined with a Gaussian fit of the mean methane mole fraction versus binned wind direction. This maximum CH_4 mole fraction was used in Equation 2 to calculate the methane emission rate Q

$$Q = 2\pi \cdot \sigma_y \cdot \sigma_z \cdot U \cdot C, \quad (2)$$

where σ_y and σ_z are the horizontal and vertical dispersion coefficients, U is the mean wind speed, and C is the maximum mole fraction from the Gaussian fit. Data quality indicators (DQIs) for this method include 3 points: (1) the location of the fitted peak methane mole fraction should agree within $\pm 30°$ with the source direction to identify possible interferences, (2) the average in-plume mole fraction enhancement should be greater than 200 ppb to ensure there was no background fluctuation, and (3) the Gaussian fit curve should correlate with the integrated measurements with an R^2 value greater than 0.80 to help identify potential interferences and obstructed wind flow conditions and to avoid collecting multiple sources in one plume (Brantley et al., 2014; Omara, 2018). Estimated emission rates were calculated using an R script, following the EPA recommendations. **Figure 2** shows an example of processed OTM-33a data as a function of the wind direction. This method was applied when the topographic conditions were appropriate (i.e., no surrounding trees or other obstacles) and when the wind conditions and measured methane mole fraction were suitable for application of OTM-33a. The uncertainty was calculated using uncertainty propagation for Equation 2 taking into account the uncertainties of the horizontal and vertical dispersion coefficients, calculated wind velocity and modeled methane mole fraction. Low precision of the geographic coordinates (3 m) determined by the GPS logger for the analyzer position represented an additional contribution to the calculation of the emission rate uncertainty, which was validated by the controlled release experiments (Korbeń, 2021).

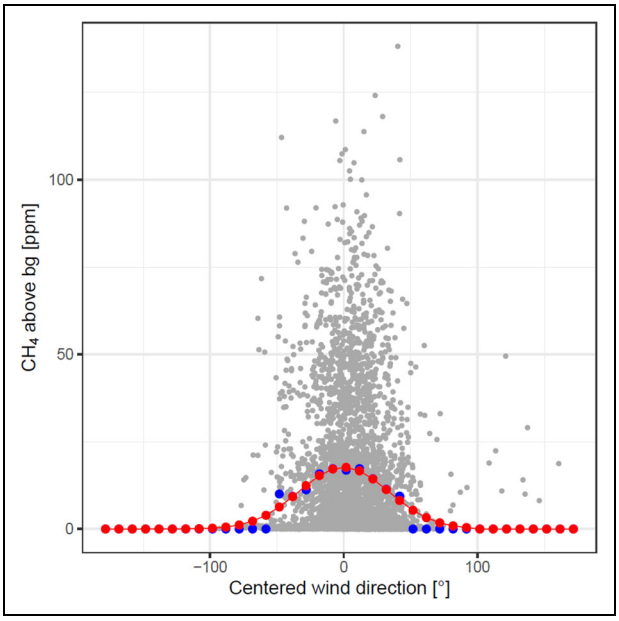

Figure 2. Example of Other Test Method 33a measurement for site ROM2563 (UHEI). CH_4 enhancement above background versus binned wind direction, where 0° corresponds to the main wind direction. The original 1-Hz CH_4 mole fractions are plotted as gray dots, the mean CH_4 mole fractions averaged over a wind direction bin of 10° as blue dots and the corresponding Gaussian fit in red.

Results and discussion

Surveyed sites

During the ROMEO campaign in October 2019, 112 different locations were visited to quantify methane emission

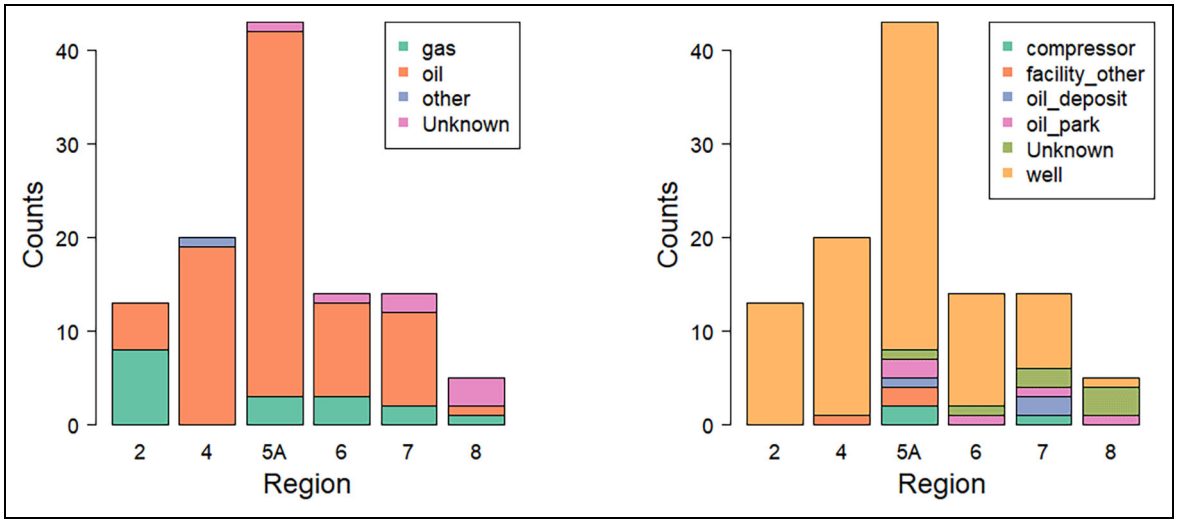

Figure 3. Distribution of quantified sites. Based on information provided by local oil and gas operator: differentiated between gas or oil (left) and type of facility, for example, oil well or other facilities (right).

rates. On those sites, OTM-33a and GPMs were applied 140 times in total (118 times OTM-33a and 22 times GPM). In order to measure as many different sites as possible, we normally visited each site only once during the campaign; 7 sites were measured several times either with different instruments/cars on different days or at different times during 1 day. They were randomly picked by usually 2 cars and estimated emission rates are considered as independent estimates.

Due to missing meteorological data, two measurements had to be rejected from further analysis. **Figure 3** shows the distribution of the surveyed sites in each region. In Region 5A, we determined the methane emission rates of 39 oil and 3 gas wells, representing 35% of quantified wells in our study. This disproportionate preference for Region 5A can be explained by the flat topography, easy access, and favorable wind conditions with stable wind speed and wind direction, compared to measurement days in other regions (see Figure S3). Wind conditions were the largest limiting factor to meet requirements for the application of the GPM or OTM-33a method. Based on meteorological forecasts, the daily average wind speed for each day between 7:00 AM and 7:00 PM at a height of 2 m did not exceed 2 m/s for half of the duration of the ROMEO campaign. In both OTM-33a and GPM applications, insufficient wind speed combined with unstable atmospheric conditions does not allow to measure methane mole fraction above the background value. These difficult conditions were encountered during mobile measurements of the ROMEO campaign. If we distinguish between different types of production infrastructure, **Figure 3** (left panel) shows that 75% of the measurements were carried out at oil wells and facilities and only 15% at gas wells, reflecting the dominance of oil production infrastructure in the target region (an actual number is listed in Table S8). Most of the studied wells were active and still pumping or collecting oil and gas (**Figure 3**, right panel).

Methane emission rate estimates with the GPM method

The GPM was applied when the OTM-33a could not be applied or when topography allowed to drive transects instead of installing the instruments on the field. In most cases, GPM was not applied for bigger facilities with several possible emitting points. On October 1, we performed a comparison measurement with the cars UHEI_1, AGH_1, and UU performing transect measurements for GPM at an oil facility. The three cars drove one after the other 10–12 transects along the road crossing the CH_4 emission plume. **Figure 4** shows two transects measured by UU and modeled using stability class B/C. All analyzed plumes show methane enhancement between 0.4 and 4.9 ppm. The emission rates estimated for this oil gathering facility from simultaneous measurements made by UHEI_1, AGH_1, and UU are 0.58 ± 0.11 kg CH_4 h^{-1}, 0.65 ± 0.07 kg CH_4 h^{-1}, and 0.68 ± 0.07 kg CH_4 h^{-1}, respectively (numbers represent the averages of individual transects ± standard error of the mean). The good agreement at this facility indicates that CH_4 emission rates derived from measurement of the different cars during the ROMEO campaign compare well.

A total of 22 GPM applications were carried out at 20 sites in all regions. Measurements from two sites were rejected during data processing, as they did not fulfill the quality criteria. The number of transects driven ranged between 5 and 22 per site. The plume crossings were performed at a distance between 11 and 160 m, and the maximal observed methane enhancement after subtracting the background was between 2 and 1,074 ppm. **Figure 5** shows the calculated methane emission rates for the 20 sites for oil wells (green), gas wells (orange), and unknown facilities (blue). The shaded area marks the results for the comparison measurements at the oil park, described above (ROM4080). The determined CH_4 emission rates vary between 0.29 ± 0.14 kg CH_4 h^{-1} and 92.9 ± 30.6 kg CH_4 h^{-1} for the individual sites, given as mean of individual transects ± standard error of the mean.

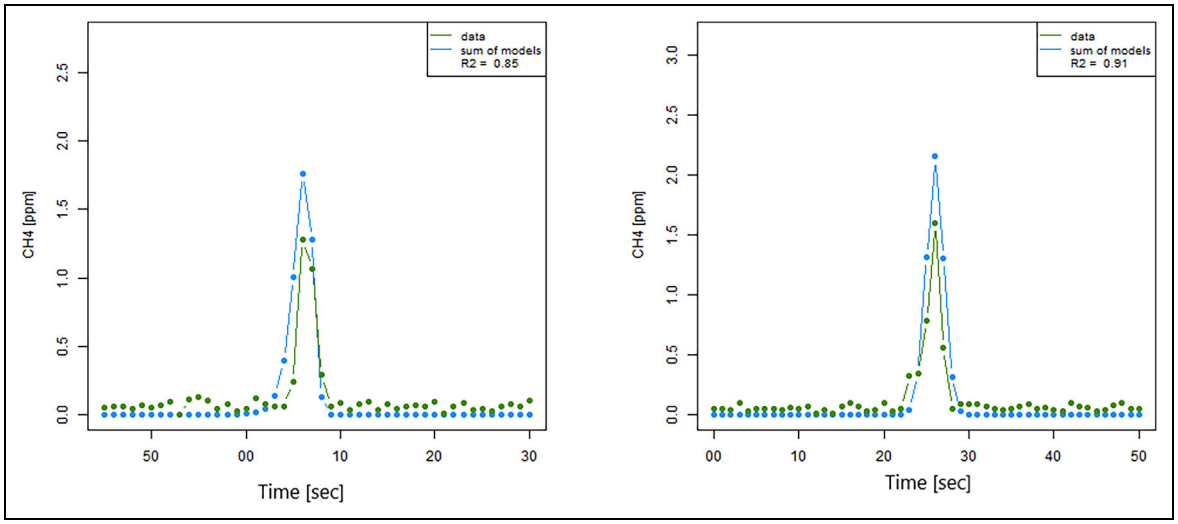

Figure 4. Example of comparison between model and data. Results for transect 2 (on the left) and 4 (on the right) for an oil park close to Prahova (measured by UU on October 1, 2019). Green dots represent measurement data, and blue dots the model output with R^2 equals 0.85 and 0.91, respectively. Note the *x*-axis is in seconds.

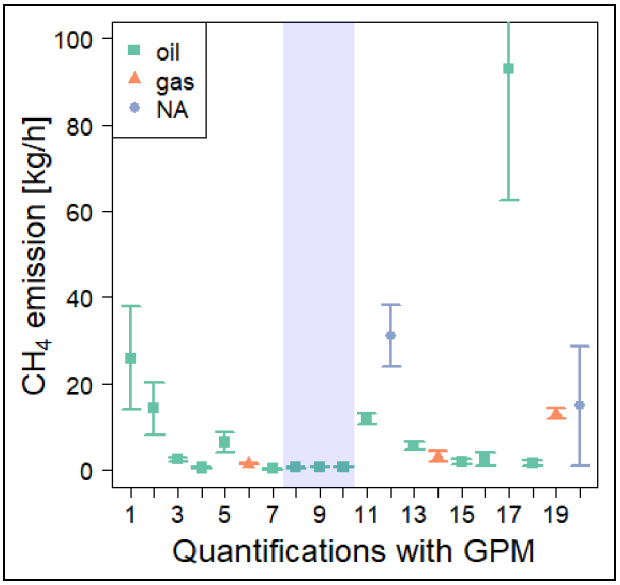

Figure 5. Calculated CH_4 emission rates for 20 sites using a Gaussian Plume Model. Green dots show emission rates for oil wells, orange for gas wells, and blue are for unknown type of the source. The shaded area marks a comparison measurement with simultaneous measurements by 3 teams (ROM4080).

Methane emission rate estimates with the OTM-33a method

OTM-33a was applied for 97 sites; 77 quantifications (65%) of the 118 OTM-33a measurements fulfill the DQIs, which is comparable to the studies of Brantley et al. (2014) and Robertson et al. (2017), where around 70% of the field measurements were accepted. Similar to the GPM evaluation, most OTM-33a measurements were applied to oil wells or facilities (**Figure 6**). Measurements for OTM-33a were performed at distances between 15 and 190 m from emitters, with an average distance of 35 m. Measured CH_4 mole fraction reached up to 1,600 ppm above ambient background, but for most sites, we measured the enhancements between 2- and 200-ppm CH_4. The calculated range of CH_4 emission rates derived with OTM-33a is comparable to the range derived from GPM results with values between 0.11 ± 0.04 kg CH_4 h^{-1} and 72.0 ± 36.4 kg CH_4 h^{-1}. Here, the uncertainty is given by the error propagation in the OTM method described above in this study.

Simultaneous OTM-33a measurements of several vehicles

During the campaign, 4 sites were measured by several cars and are marked by shaded area on **Figure 6** and Table S6. The first field comparison of OTM-33a was performed at well number ROM2090 by the cars UHEI_1 and AGH_1. Both methane analyzers were installed in the field at a distance of 46 and 43 m from the gas well, respectively. The measured CH_4 enhancements were similar, resulting in a very good agreement of the CH_4 emission rates with 0.61 ± 0.25 kg CH_4 h^{-1} for each instrument. A second comparison was carried out at well number ROM2563 (gas well) on November 3, UHEI_1 and AGH_1 measured simultaneously using the OTM-33a method, and estimated CH_4 emission rates in good agreement of 15.4 ± 6.0 kg CH_4 h^{-1} and 14.7 ± 5.7 kg CH_4 h^{-1}, respectively.

Multiple measurements at selected sites

Three selected sites have been visited on several days during the measurement campaign to gain statistical data on the variability of CH_4 emission rates. All measured CH_4 emission rates are summarized in Table S7. Six measurements were taken at site ROM1474 on 3 days between October 14 and 18. The CH_4 emission rates varied between 0.4 and 3.6 kg CH_4 h^{-1} around a mean value of 1.9 ± 1.12 kg CH_4/h. A similar variability between measurement days was found at ROM4625 and ROM5688, with CH_4 emission range between 0.8 and 1.7 kg CH_4/h^{-1} and 0.9 and 1.9 kg CH_4 h^{-1}.

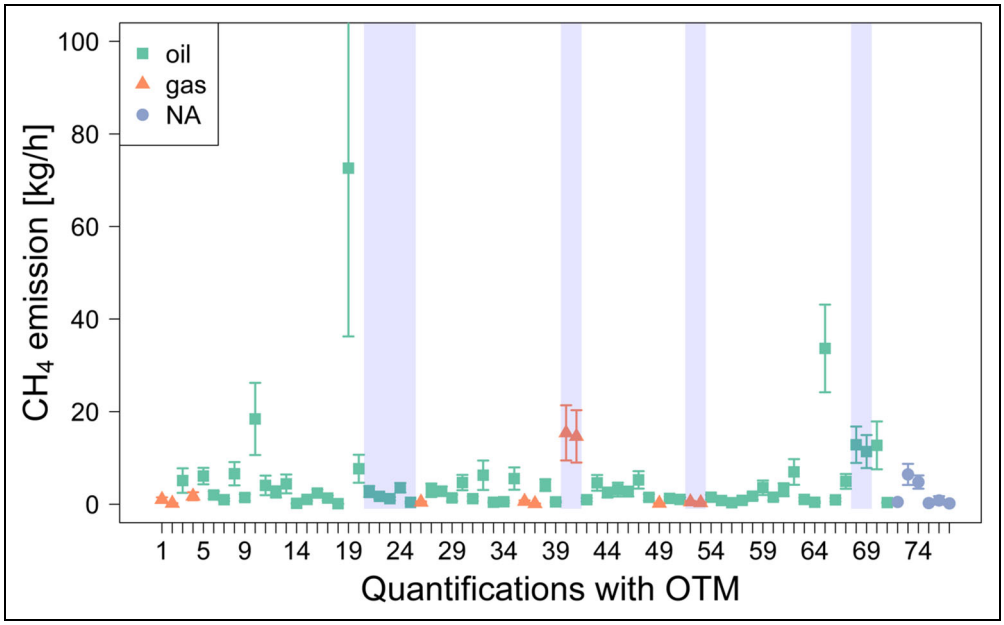

Figure 6. Calculated emission rates by Other Test Method 33a (OTM-33a). Green, orange, and blue dots represent CH_4 emission rates for oil, gas, and unknown type of the source site, respectively. The shaded areas mark sites with several application of OTM-33a.

A different behavior shows ROM2563, with a very high emission rate of around 15 kg CH_4 h^{-1} measured on November 3. The second measurement at ROM2563 on November 9 showed already during measurements much smaller CH_4 enhancements. The use of the GPM method at the end of the measurement campaign estimated the emission rates of 1.5 $\pm$ 0.3 kg CH_4 h^{-1}, which is a factor 10 lower than the first approach. This decrease in CH_4 emission rate can be explained by the intervention of a service team from the operator, which repaired a leak after we reported the large CH_4 emission rates. It should be mentioned that the determined emission rates are only a snapshot during our measurement campaign. However, multiple measurements at selected sites can give an indication of the temporal variability during the campaign.

Emission rates below the detection limit

The screening data were used for estimating emission rates that are below the detection limit of the OTM-33a method. Some sites where the screening cars were clearly downwind were detected with no methane enhancements or the CH_4 enhancement was below 200 ppb and therefore below the limit for OTM-33a. Those sites were marked in a table as BG (background) or with the measured mole fraction up to 2.2-ppm CH_4, respectively. All screening measurements were performed within 8–30 m of the source. Brantley et al. (2014) determined the lower detection limit of the OTM-33a method as 0.036 kg CH_4 h^{-1}, which corresponded to a downwind average in-plume CH_4 excess greater than 100 ppb. In this study, the lowest emission rate determined was 0.11 $\pm$ 0.04 kg CH_4 h^{-1}.

Similar to the study of Robertson et al. (2020), we also calculated the number of oil and gas wells that are below the detection limit in order to include them in the representative estimates for the regions. However, we used the much larger database of screening data instead of the quantified sites only. We have chosen the screening data measured by vehicles UHEI_1 and UHEI_2, as the documentation on files was the most complete. In total, 532 screening of wells were performed by the two cars equipped with instrumentation of Heidelberg University; 42 of these measurements could only be carried out upwind the well or had other invalid entries in the comment column and were therefore not used for further evaluations. In addition, we excluded the 28 sites which were classified as "disposal_injection" as we have not quantified any of this site types. Of the 462 remaining screening data, 98 were flagged as "BG" (background, indicating no discernible CH_4 elevation), and 61 had a low mole fraction excess of 0.050–0.29 ppm. These 159 sites from screening dataset that are below our detection limit (BDL) for the OTM-33a method correspond to a proportion of 35%. This percentage of emission rates below the detection limit is comparable to the result of Robertson et al. (2020), who found a share of 38% in a study of CH_4 emissions of oil and gas wells in New Mexico. We have investigated the sensitivity of calculating this fraction by using different scenarios with subsets of our data, such as screenings performed by the UHEI_1 or UHEI_2 car, and the result varies only minimally between 34% and 36%.

However, the number of sites below detection limit varies significantly between the regions and also between oil and gas wells. The proportion of measurements below the detection limit is 35% for oil wells and 22% for gas wells. The differences between the regions reflect partly the share of the oil and gas wells in the investigated regions (Table S8). Since we screened a much lower number of gas wells (6% of all screenings), it is unclear whether this distinction is robust; however, the dominance of oil facilities over gas facilities reaches over

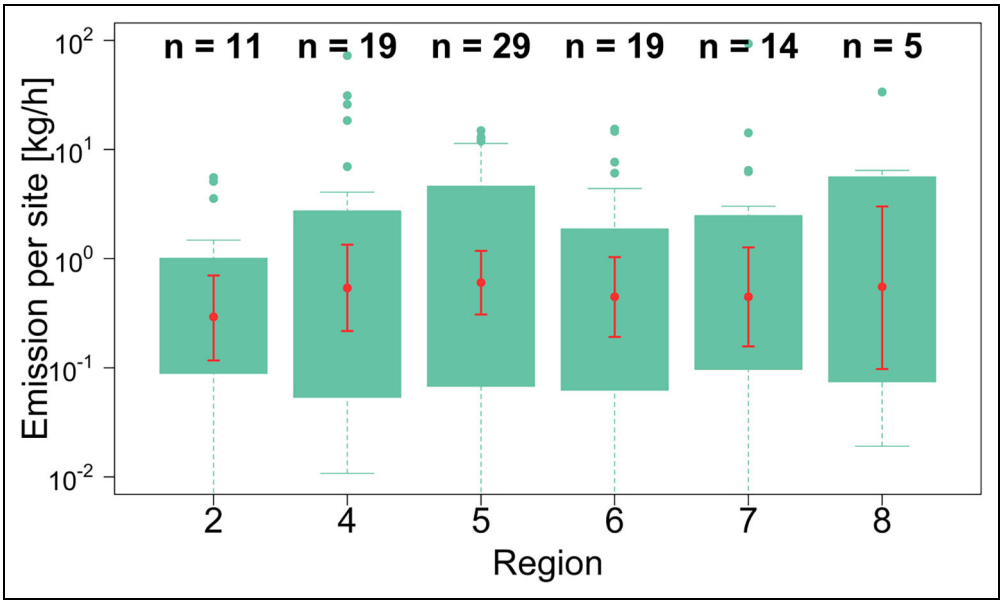

Figure 7. Comparison of derived methane emission rates by region. Boxes represent the first and third quartile of the data, while whiskers extend to the largest value that is within 1.5 times the interquartile range. Means and 95% confidence intervals are shown in red and were calculated using a nonparametric bootstrap method. Data are presented on a logarithmic *y*-axis. The number of accepted quantifications per region is displayed in the top line. This graph includes 35% of the nondetects as described in the section "Emission rates below the detection limit."

85% for most of the investigated regions (Table S8). Therefore, we applied a mean factor of nondetects of 35% to all regions and all types of wells and facilities. To estimate emission rates from these nondetect sites, values between 0 kg CH_4/h and our lowest determined value of 0.11 kg CH_4 h^{-1} were randomly assigned with equal probability similar to Robertson et al. (2020).

Comparison of estimated methane emission rates for regions and type of visited sites

In **Figures 7** and **8**, we show the determined CH_4 emission rates separately for each region as well as for each status of production. Using a nonparametric bootstrap method (resampling of the data set of all quantifications including 35% of BDL, $R = 10{,}000$), the mean and the 95% CI for the logarithmic scale were calculated and then expressed in the kg/h units.

The mean methane emission rates with 95% CIs for a given region vary between 0.29 and 0.60 kg CH_4 h^{-1} per site for Region 2 and Region 5A, respectively. All data are summarized in **Table 2**.

The lowest CH_4 emission rates with 0.29 kg CH_4 h^{-1} were found in Region 2. However, the number of sites measured per region varies significantly between 5 and 29, and thus, the CI values also have a wider range for Region 8, which has the smallest number of accepted quantifications ($n = 5$). Regions 2 and 8 have a larger share of gas wells with 40% and 56% compared to other regions with only up to 15% of gas wells (numbers of oil and gas wells in each region are provided in Table S8). The lower CH_4 emission rates in Region 2 are in line with our results for gas wells (**Figure 8**), as methane is the main product and not an associated gas as for the oil extraction where usually more equipment per site (and thus potential emission sources) is present.

Figure 8 presents the distribution of methane emission rates separated by production status (top panel) and the gas or oil type (lower panel) of the emitter. The number of nonproducing wells is very small and statistically not significant. However, it has been shown that the 19 highest emission rates (20%) were measured from wells that were still producing. When comparing the well type (**Figure 8**, bottom panel), higher average emission rates are indicated by the oil wells, however—as mentioned before—a larger number of quantifications were completed for them. The average emission rates per site are estimated to be 0.53 [0.35, 0.82] kg CH_4 h^{-1} and 0.35 [0.15, 0.84] kg CH_4 h^{-1} for oil and gas related facilities, respectively.

Comparison to other studies

The estimated emission rates during the ROMEO campaign, including the calculation for the emission rates below the detection limit varied between 0.01 kg CH_4 h^{-1} and 93.6 kg CH_4 h^{-1} for a single site, with mean and with a 95% CI value equal to 0.49 [0.35, 0.71] kg CH_4 h^{-1} per site. The mean methane emission rate with 95% CIs for oil sites was 0.53 [0.35, 0.82] kg CH_4 h^{-1}, while for gas wells, it was 0.35 [0.15, 0.84] kg CH_4 h^{-1}. Repeated measurements at some sites (see above) show steady emissions. It is worth mentioning here the possibility of time variability in the emission rates, however, there are also cases where a significant drop in emission rate has been found after remedial intervention.

During the ROMEO campaign, a second study with ground-based measurements using a tracer gas dispersion method was carried out by Delre et al. (2022). They

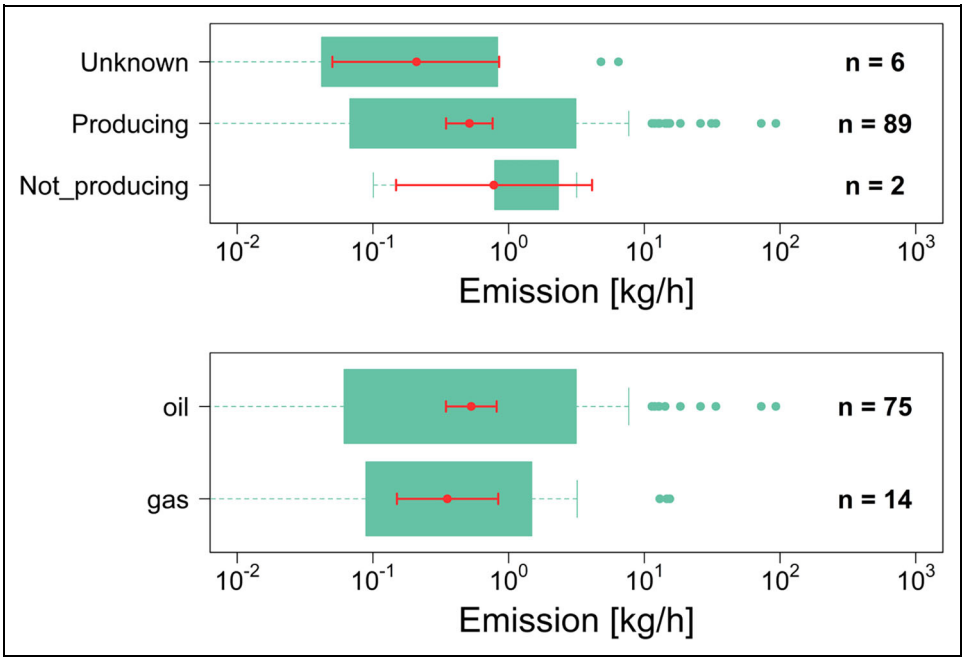

Figure 8. Estimated emission rates distributed by status (on the top) and type (on the bottom) of the quantified site. Means and 95% confidence intervals are shown in red and were calculated using a nonparametric bootstrap method. Note the logarithmic *x*-axis. The number of accepted quantifications per status or type is indicated on the right side. This graph includes 35% of the nondetects as described in the section "Emission rates below the detection limit."

Table 2. Mean methane emission rates with 95% confidence intervals for the different regions including 35% of the nondetects

Region	Mean Methane Emission Rate (kg CH_4 h^{-1})	95% Confidence Intervals (kg CH_4 h^{-1})	Number of Accepted Quantifications Per Region (Without BDL)
2	0.29	[0.12, 0.70]	11
4	0.54	[0.22, 1.34]	19
5A	0.60	[0.31, 1.18]	29
6	0.45	[0.19, 1.03]	19
7	0.45	[0.16, 1.27]	14
8	0.55	[0.10, 3.01]	5

BDL = below our detection limit.

focused more on the Regions 6 and 7 around the city of Ploiesti (see **Figure 1**), while this study also measured in Regions 2, 4 and 5A, west of Bucharest. The CH_4 emission rates from the oil and gas sector in Romania are very similar in both studies with 0.49 [0.35, 0.71] kg CH_4 h^{-1} per site in this study and 0.53 [0.32, 0.79] kg CH_4 h^{-1} per site in Delre et al. (2022). The contribution of the high emitter was comparable, with 10% of the sites contributing to 56% of the total CH_4 emission rate in this study, compared to 5% of the sites contributing to 52% of the total CH_4 emission rate in Delre et al. (2022).

Emissions from the oil and gas industry have been the subject of many studies in recent years (Brantley et al., 2014; Mitchell et al., 2015; Zavala-Araiza et al., 2015; Atherton et al., 2017; Robertson et al., 2017; Omara et al., 2018; Robertson et al., 2020). In a study published by Robertson et al. (2017), methane emissions from four major U.S. basins were examined: Upper Green River (UPR), Denver-Julesburg (DJ), Uintah, and Fayetteville (FV). Measurements were made using the OTM-33a method and upscaled emissions for pads were presented. Estimated methane emission ranges of 95% CIs per site are in the range of 0.38–3.1 kg CH_4 h^{-1} for UPR, DJ, and FV. For Uintah, it is 0.8–9.1 kg CH_4 h^{-1}. A study by Brantley et al. (2014) found these values to be 0.40–2.66 kg CH_4 h^{-1} for samples from the Barnett, DJ, and Pinedale basins, respectively. A recent study from the Permian Basin (United States) published by Robertson et al. (2020) shows emission rates (95% CI) of 0.70–7.61 kg CH_4 h^{-1}.

The CH_4 emission rates from U.S. oil and gas basins are comparable to the methane emission rates obtained during the ROMEO campaign. However, it should be taken into account that each of the basins in the United States are very large, up to the size of Romania for a single basin. Furthermore, the number of visited sites using the screening cars represents already 17% of the total sites reported by local O&G operator. The combined evidence from quantification and screening should provide a realistic impression of methane emissions from the oil and gas industry in Romania. It should be noted that the ROMEO campaign was focused on the southern part of the country, while oil and gas deposits also exist in other parts of Romania

including in Transylvania, western Romania, and in the Black Sea, most of which has not been studied in detail so far. During the finalization of this article, the ROMEO team has completed ground-based measurements in Transylvania, which will be analyzed and published later. A future analysis will synthesize all empirical ground-based measurement data to provide a more comprehensive picture of O&G-related methane emissions in Romania including a comparison with national greenhouse gas inventory data.

Data accessibility statement

The emission data set associated with this submission is partly presented in Table S7. More detailed information is accessible on the request to the corresponding author.

Supplemental files

The supplemental files for this article can be found as follows:

Figures S1–S3. Tables S1– S8. Docx

Acknowledgments

We acknowledge the German Environment Agency (Umweltbundesamt—UBA), which has provided their CRDS Analyser G1301 for 3 weeks of mobile measurements in Romania. The Other Test Method 33a code was written by Environmental Protection Agency team and provided to UHEI team. The analysis was made by R code. All mobile measurements were performed and supported by Romanian partners: Calin Baciu, Andreea Calcan, Magdalena Ardelean, Alexandru Mereuta, Horatiu Stefanie, Tudor Alexandru, Sebastian Iancu, and Marius Corbu. For the publication fee, we acknowledge financial support by Deutsche Forschungsgemeinschaft within the funding program "Open Access Publikationskosten" as well as by Heidelberg University.

Funding

These surveys were funded by the ROmanian Methane Emissions from Oil and gas (ROMEO) project, funded by the Climate and Clean Air Coalition (CCAC) of UNEP under grant number PCA/CCAC/UU/DTIE19-EN652. The ROMEO campaign was initiated by the European H2020 project MEMO2, which has received funding from the European Union's Horizon 2020 research and innovation program under the Marie Sklodowska-Curie grant agreements No. 722479. The part of research results presented in this article has been developed with the use of equipment financed from the funds of the "Excellence Initiative—Research University" program at AGH University of Science and Technology.

Competing interests

The authors have no competing interests, as defined by Elementa, which might be perceived to influence the research presented in this article.

Author contributions

The manuscript was written by PK, MS, and PJ. PK, PJ, MS, JMN, and JB were responsible for data processing and analysis. PK, PJ, HM, and AR collected and provided data for quantifications. PK, PJ, HM, AR, JB, MS, and JMN made screening before one of the method was applied. All authors have given approval to the final version of the manuscript. MS, JMN, and TR gave scientific correction.

References

Allen, DT. 2016. Emissions from oil and gas operations in the United States and their air quality implications. *Journal of the Air & Waste Management Association* **66**(6): 549–575. DOI: http://doi.org/10.1080/10962247.2016.1171263.

Ars, S, **Broquet, G**, **Kwok, CY**, **Roustan, Y**, **Wu, L**, **Arzoumanian, E**, **Bousquet, P.** 2017. Statistical atmospheric inversion of local gas emissions by coupling the tracer release technique and local transport modelling: A test case with controlled methane emissions. *Atmospheric Measurement Techniques* **10**(12): 5017–5037. DOI: http://doi.org/10.5194/amt-10-5017-2017.

Atherton, E, **Risk, D**, **Fougère, C**, **Lavoie, M**, **Marshall, A**, **Werring, J**, **Williams, JP**, **Minions, C.** 2017. Mobile measurement of methane emissions from natural gas developments in northeastern British Columbia, Canada. *Atmospheric Chemistry and Physics* **17**: 12405–12420. DOI: http://doi.org/10.5194/acp-17-12405-2017.

BasicAirData GPS Logger. Available at www.basicairdata.eu/projects/android/android-gps-logger/. Accessed 28 July 2022.

Brantley, HL, **Thoma, ED**, **Squier, WC**, **Guven, BB**, **Lyon, D.** 2014. Assessment of methane emissions from oil and gas production pads using mobile measurements. *Environmental Science & Technology* **48**: 14508–14515. DOI: http://doi.org/10.1021/es503070q.

Cain, M, **Warwick, NJ**, **Fisher, RE**, **Lowry, D**, **Lanoiselle, M**, **Nisbet, EG**, **France, J**, **Pitt, J**, **O'Shea, S**, **Bower, K**, **Allen, G**, **Illingworth, S**, **Manning, AJ**, **Bauguitte, S**, **Pisso, I**, **Pyle, JA.** 2017. A cautionary tale: A study of a methane enhancement over the North Sea. *Journal of Geophysical Research Atmospheres* **122**(14): 7630–7645. DOI: http://doi.org/10.1002/2017JD026626.

Caulton, DR, **Li, Q**, **Bou-Zeid, E**, **Fitts, JP**, **Golston, LM**, **Pan, D**, **Lu, J**, **Lane, HM**, **Buchholz, B**, **Guo, X**, **McSpiritt, J**, **Wendt, L**, **Zondlo, MA.** 2018. Quantifying uncertainties from mobile-laboratory-derived emissions of well pads using inverse Gaussian methods. *Atmospheric Chemistry and Physics* **18**: 15145–15168. DOI: http://doi.org/10.5194/acp-18-15145-2018.

Delre, A, **Hensen, A**, **Velzeboer, I**, **van den Bulk, P**, **Edjabou, ME**, **Scheutz, C.** 2022. Methane and ethane emission quantifications from onshore oil and gas sites in Romania, using a tracergas dispersion method. *Elementa: Science of the Anthropocene* **10**: 1. DOI: http://doi.org/10.1525/elementa.2021.000111.

Dlugokencky, EJ, **Myers, RC**, **Lang, PM**, **Masarie, KA**, **Crotwell, AM**, **Thoning, KW**, **Hall, BD**, **Elkins, JW**, **Steele, LP.** 2005. Conversion of NOAA atmospheric dry air CH_4 mole fractions to a gravimetrically prepared standard scale. *JGR-Atmospheres* **110**: D18. DOI: http://doi.org/10.1029/2005JD006035.

Edie, R, **Robertson, AM**, **Field, RA**, **Soltis, J**, **Snare, DA**, **Zimmerle, D**, **Bell, CS**, **Vaughn, TL**, **Murphy, SM.** 2020. Constraining the accuracy of flux estimates using OTM 33A. *Atmospheric Measurement Techniques* **13**: 341–353. DOI: http://doi.org/10.5194/amt-13-341-2020.

GasScouter™ G4301. 2021. Analyzer datasheet. Available at www.picarro.com. Accessed 28 July 2022.

Griffiths, RF. 1994. Errors in the use of the Briggs parametrization for atmospheric dispersion coefficients. *Atmospheric Environment* **28**(17): 2861–2865. DOI: http://doi.org/10.1016/1352-2310(94)90086-8.

Hanna, SR, **Briggs, GA**, **Hosker, RP**, Jr. 1982. *Handbook on atmospheric diffusion (No. DOE/TIC-11223)*. Oak Ridge, TN: National Oceanic and Atmospheric Administration. DOI: http://doi.org/10.2172/5591108.

Hmiel, B, **Petrenko, VV**, **Dyonisius, MN**, **Buizert, C**, **Smith, AM**, **Place, PF**, **Harth, C**, **Beaudette, R**, **Hua, Q**, **Yang, B**, **Vimont, I**, **Michel, SE**, **Severinghaus, JP**, **Etheridge, D**, **Bromley, T**, **Schmitt, J**, **Fain, X**, **Weiss, RF**, **Dlugokencky, E.** 2020. Preindustrial $^{14}CH_4$ indicates greater anthropogenic fossil CH_4 emissions. *Nature* **578**: 409–412. DOI: http://doi.org/10.1038/s41586-020-1991-8.

Intergovernmental Panel on Climate Change. 2021. Climate change 2021: The physical science basis, in Masson-Delmotte, V, Zhai, P, Pirani, A, Connors, SL, Péan, C, Berger, S, Caud, N, Chen, Y, Goldfarb, L, Gomis, MI, Huang, M, Leitzell, K, Lonnoy, E, Matthews, JBR, Maycock, TK, Waterfield, T, Yelekçi, O, Yu, R, Zhou, B eds., *Contribution of Working Group I to the sixth assessment report of the Intergovernmental Panel On Climate Change*. Cambridge: Cambridge University Press.

International Energy Agency. 2017. World energy outlook. Available at https://www.iea.org/reports/world-energy-outlook-2017. Accessed 28 July 2022.

Kammerer, J. 2019. A study of controlled methane release experiments for emissions quantification with an application to a dairy farm [Master's thesis]. Heidelberg, Germany: Heidelberg University.

Korbeń, P. 2021. Estimation of methane emission and investigation of isotopic composition of methane from selected source in Germany, Poland and Romania [Ph.D. dissertation]. Heidelberg, Germany: Heidelberg University. DOI: http://doi.org/10.11588/heidok.00030547.

Kumar, F, **Broquet, G**, **Yver-Kwok, C**, **Laurent, O**, **Gichuki, S**, **Caldow, C**, **Cropley, F**, **Lauvaux, T**, **Ramonet, M**, **Berthe, G**, **Martin, F**, **Duclaux, O**, **Juery, C**, **Bouchet, C**, **Ciais, P.** 2021. Mobile atmospheric measurements and local-scale inverse estimation of the location and rates of brief CH_4 and CO_2 releases from point sources. *Atmospheric Measurement Techniques* **14**: 5987–6003. DOI: http://doi.org/10.5194/amt-14-5987-2021.

Lauvaux, T, **Giron, C**, **Mazzolini, M**, **d'Aspremont, A**, **Duren, R**, **Cusworth, D**, **Shindell, D**, **Ciais, P.** 2022. Global assessment of oil and gas methane ultra-emitters. *Science* **375**(6580): 557–561. DOI: http://doi.org/10.1126/science.abj4351.

LGR Manual. 2019 Oct. LGR-ICOS™ GLA131 Greenhouse gas analyzer—Data sheet. Available at https://www.lgrinc.com/documents/DS_LGR-ICOS_MGGA_MGPC-EN%20RevD.pdf. Accessed 28 July 2022.

Licor Manual. 2022 Jul. LI-7810 $CH_4/CO_2/H_2O$ Trace gas analyzer—Instruction manual. Available at https://www.licor.com/documents/zsce2z88fgkfpbiguqi0k3g537jllsl7. Accessed 28 July 2022.

Menoud, M, **van der Veen, C**, **Maazallahi, H**, **Hensen, A**, **Velzeboer, I**, **van den Bulk, P**, **Delre, A**, **Korbeń, P**, **Schwietzke, S**, **Ardelean, M**, **Calcan, A**, **Etiope, G**, **Baciu, C**, **Scheutz, C**, **Schmidt, M**, **Röckmann, T.** 2022. CH_4 isotopic signatures of emissions from oil and gas extraction sites in Romania. *Elementa: Science of the Anthropocene* **10**: 1. DOI: http://doi.org/10.1525/elementa.2021.00092.

Mitchell, AL, **Tkacik, DS**, **Roscioli, JR**, **Herndon, SC**, **Yacovitch, TI**, **Martinez, DM**, **Vaughn, TL**, **Williams, LL**, **Sullivan, MR**, **Floerchinger, C**, **Omara, M**, **Subramanian, R**, **Zimmerle, D**, **Marchese, AJ**, **Robinson, AL.** 2015. Measurements of methane emissions from natural gas gathering facilities and processing plants: Measurement results. *Environmental Science & Technology* **49**(5): 3219–3227. DOI: http://doi.org/10.1021/es5052809.

Mønster, JG, **Samuelsson, J**, **Kjeldsen, P**, **Rella, CW**, **Scheutz, C.** 2014. Quantifying methane emission from fugitive sources by combining tracer release and downwind measurements—A sensitivity analysis based on multiple field surveys. *Waste Management* **34**(8): 1416–1428. DOI: http://doi.org/10.1016/j.wasman.2014.03.025.

Ocko, IB, **Sun, T**, **Shindell, D**, **Oppenheimer, M**, **Hristov, AN**, **Pacala, SW**, **Mauzerall, DL**, **Xu, Y**, **Hamburg, SP.** 2021. Acting rapidly to deploy readily available methane mitigation measures by sector can immediately slow global warming. *Environmental Research Letters* **16**(5): 054042. DOI: http://doi.org/10.1088/1748-9326/abf9c8.

Omara, M. 2018. Methane emissions measurements and quantification using EPA's Other Test Method (OTM) 33a [pdf presentation]. Environmental Defense Fund, Austin, TX.

Omara, M, **Zimmerman, N**, **Sullivan, MR**, **Li, X**, **Ellis, A**, **Cesa, R**, **Subramanian, R**, **Presto, AA**, **Robinson, AL.** 2018. Methane emissions from natural gas production sites in the United States: Data synthesis and national estimate. *Environmental Science & Technology* **52**(21): 12915–12925. DOI: http://doi.org/10.1021/acs.est.8b03535.

Paris, J-D, **Riandet, A**, **Bourtsoukidis, E**, **Delmotte, M**, **Berchet, A**, **Williams, J**, **Ernle, L**, **Tadic, I**, **Harder, H**, **Lelieveld, J.** 2021. Shipborne measurements of methane and carbon dioxide in the Middle East and Mediterranean areas and the contribution from oil and gas emissions. *Atmospheric Chemistry and Physics* **21**: 12443–12462. DOI: http://doi.org/10.5194/acp-21-12443-2021.

Ravikumar, AP, **Roda-Stuart, D**, **Liu, R**, **Bradley, A**, **Bergerson, J**, **Nie, Y**, **Zhang, S**, **Bi, X**, **Brandt, AR.** 2020. Repeated leak detection and repair surveys reduce methane emissions over scale of years. *Environmental Research Letters* **15**: 034029. DOI: http://doi.org/10.1088/1748-9326/ab6ae1.

Robertson, AM, **Edie, R**, **Field, RA**, **Lyon, D**, **McVay, R**, **Omara, M**, **Zavala-Araiza, D**, **Murphy, SM.** 2020. New Mexico Permian Basin measured well pad methane emissions are a factor of 5-9 times higher than U.S. EPA estimates. *Environmental Science & Technology* **54**: 13926–13934. DOI: http://doi.org/10.1021/acs.est.0c02927.

Robertson, AM, **Edie, R**, **Snare, D**, **Soltis, J**, **Field, RA**, **Burkhart, MD**, **Bell, CS**, **Zimmerle, D**, **Murphy, SM.** 2017. Variation in methane emission rates from well pads in four oil and gas basins with contrasting production volumes and compositions. *Environmental Science & Technology* **51**(15): 8832–8840. DOI: http://doi.org/10.1021/acs.est.7b00571.

Saunois, M, **Stavert, AR**, **Poulter, B**, **Bousquet, P**, **Canadell, JG**, **Jackson, RB**, **Raymond, PA**, **Dlugokencky, EJ**, **Houweling, S**, **Patra, PK**, **Ciais, P**, **Arora, VK**, **Bastviken, D**, **Bergamaschi, P**, **Blake, DR**, **Brailsford, G**, **Bruhwiler, L**, **Carlson, KM**, **Carrol, M**, **Castaldi, S**, **Chandra, N**, **Crevoisier, C**, **Crill, PM**, **Covey, K**, **Curry, CL**, **Etiope, G**, **Frankenberg, C**, **Gedney, N**, **Hegglin, MI**, **Höglund-Isaksson, L**, **Hugelius, G**, **Ishizawa, M**, **Ito, A**, **Janssens-Maenhout, G**, **Jensen, KM**, **Joos, F**, **Kleinen, T**, **Krummel, PB**, **Langenfelds, RL**, **Laruelle, GG**, **Liu, L**, **Machida, T**, **Maksyutov, S**, **McDonald, KC**, **McNorton, J**, **Miller, PA**, **Melton, JR**, **Morino, I**, **Müller, J**, **Murguia-Flores, F**, **Naik, V**, **Niwa, Y**, **Noce, S**, **O'Doherty, S**, **Parker, RJ**, **Peng, C**, **Peng, S**, **Peters, GP**, **Prigent, C**, **Prinn, R**, **Ramonet, M**, **Regnier, P**, **Riley, WJ**, **Rosentreter, JA**, **Segers, A**, **Simpson, IJ**, **Shi, H**, **Smith, SJ**, **Steele, LP**, **Thornton, BF**, **Tian, H**, **Tohjima, Y**, **Tubiello, FN**, **Tsuruta, A**, **Viovy, N**, **Voulgarakis, A**, **Weber, TS**, **van Weele, M**, **van der Werf, GR**, **Weiss, RF**, **Worthy, D**, **Wunch, D**, **Yin, Y**, **Yoshida, Y**, **Zhang, W**, **Zhang, Z**, **Zhao, Y**, **Zheng, B**, **Zhu, Q**, **Zhu, Q**, **Zhuang, Q.** 2019. The global methane budget 2000–2017. *Earth System Science Data Discuss* **12**: 1561–1623. DOI: http://doi.org/10.5194/essd-2019-128.

Schwietzke, S, **Sherwood, O**, **Bruhwiler, L**, **Miller, JB**, **Etiope, G**, **Dlugokencky, EJ**, **Englund Michel, S**, **Arling, VA**, **Vaughn, BH**, **White, JWC**, **Tans, PP.** 2016. Upward revision of global fossil fuel methane emissions based on isotope database. *Nature* **538**: 88–91. DOI: http://doi.org/10.1038/nature19797.

Shen, L, **Zavala-Araiza, D**, **Gautam, R**, **Omara, M**, **Scarpelli, T**, **Sheng, J**, **Sulprizio, MP**, **Zhuang, J**, **Zhang, Y**, **Qu, Z**, **Li, X**, **Hamburg, SP**, **Jacob, DJ.** 2021. Unravelling a large methane emission discrepancy in Mexico using satellite observation. *Remote Sensing of Environment* **260**: 112461. DOI: http://doi.org/10.1016/j.rse.2021.112461.

Solazzo, E, **Crippa, M**, **Guizzardi, D**, **Muntean, M**, **Choulga, M**, **Janssens-Maenhout, G.** 2021. Uncertainties in the Emissions Database for Global Atmospheric Research (EDGAR) emission inventory of greenhouse gases. *Atmospheric Chemistry and Physics* **21**: 5655–5683. DOI: http://doi.org/10.5194/acp-21-5655-2021.

Thoma, ED, **Brantley, H**, **Squier, B**, **DeWees, J**, **Segall, R**, **Merrill, R.** 2015. Development of mobile measurement method series OTM33, in *Proceedings, 108th Annual Conference of the Air & Waste Management Association*, Raleigh, NC, June 23–26. Pittsburgh, PA: Air and Waste Management Association: 999. Available at https://cfpub.epa.gov/si/si_public_record_report.cfm?Lab=NRMRL&dirEntryId=320210.

Thoma, ED, **Squier, B.** 2014. OTM 33 geospatial measurement of air pollution, Remote Emissions Quantification (GMAP-REQ) and OTM33A Geospatial Measurement of Air Pollution-Remote Emissions Quantification-Direct Assessment (GMAP-REQ-DA). Cincinnati, OH: U.S. Environmental Protection Agency. Available at http://www3.epa.gov/ttnemc01/prelim/otm33.pdf.

Turner, DB. 1970. *Workbook of atmospheric dispersion estimates (Office of Air Program Pub. No. AP-26)*. Washington, DC: Environmental Protection Agency.

Tyner, DR, **Johnson, MR.** 2021. Where the methane is—Insights from Novel Airborne LiDAR measurements combined with ground survey data. *Environmental Science & Technology* **55**(14): 9773–9783. DOI: http://doi.org/10.1021/acs.est.1c01572.

U.S. Environmental Protection Agency. 2016. Inventory of U.S. greenhouse gas emissions and sinks: 1990–2014. EPA 430-R-16-002. Available at https://www.epa.gov/ghgemissions/inventory-us-greenhouse-gas-emissions-and-sinks-1990-2014.

Yacovitch, TI, **Herndon, SC**, **Pétron, G**, **Kofler, J**, **Lyon, D**, **Zahniser, MS**, **Kolb, CE.** 2015. Mobile laboratory observations of methane emissions in the Barnett Shale Region. *Environmental Science & Technology* **49**(13): 7889–7895. DOI: http://doi.org/10.1021/es506352j.

Yacovitch, TI, **Neininger, B**, **Herndon, SC**, **van der Gon, HD**, **Jonkers, S**, **Hulskotte, J**, **Roscioli, JR**, **Zavala-Araiza, D.** 2018. Methane emissions in the Netherlands: The Groningen field. *Elementa: Science of the Anthropocene* **6**: 57. DOI: http://doi.org/10.1525/elementa.308.

Zavala-Araiza, D, **Herndon, SC**, **Roscioli, JR**, **Yacovitch, TI**, **Johnson, MR**, **Tyner, DR**, **Omara, M**, **Knighton, B.** 2018. Methane emissions from oil and gas

production sites in Alberta, Canada. *Elementa: Science of the Anthropocene* **6**: 27. DOI: http://doi.org/10.1525/elementa.284.

Zavala-Araiza, D, **Lyon, D**, **Alvarez, RA**, **Palacios, V**, **Harriss, R**, **Lan, X**, **Talbot, R**, **Hamburg, SP.** 2015. Toward a functional definition of methane super-emitters: Application to natural gas production sites. *Environmental Science & Technology* **49**(13): 8167–8174. DOI: http://doi.org/10.1021/acs.est.5b00133.

How to cite this article: Korbeń, P, Jagoda, P, Maazallahi, H, Kammerer, J, Nęcki, JM, Wietzel, JB, Bartyzel, J, Radovici, A, Zavala-Araiza, D, Röckmann, T, Schmidt, M. 2022. Quantification of methane emission rate from oil and gas wells in Romania using ground-based measurement techniques. *Elementa: Science of the Anthropocene* 10(1). DOI: https://doi.org/10.1525/elementa.2022.00070

Domain Editor-in-Chief: Detlev Helmig, Boulder AIR LLC, Boulder, CO, USA

Guest Editor: David Lowry, Royal Holloway University of London, Egham, United Kingdom

Knowledge Domain: Atmospheric Science

Part of an Elementa Special Feature: Oil and Natural Gas Development: Air Quality, Climate Science, and Policy

Published: November 16, 2022 **Accepted:** September 29, 2022 **Submitted:** May 23, 2022

ELEMENTA Science of the Anthropocene

Elem Sci Anth is a peer-reviewed open access journal published by University of California Press.

OPEN ACCESS